Fracture Mechanics of Concrete Structures
Proceedings FRAMCOS-3
AEDIFICATIO Publishers, D-79104 Freiburg, Germany

APPLICATION OF PSEUDO STRAIN HARDENING CEMENTITIOUS COMPOSITES TO SHEAR RESISTANT STRUCTURAL ELEMENTS

T. Kanda and S. Watanabe
Kajima Technical Research Institute, Japan
V. C. Li
ACE-MRL, Department of Civil and Environmental Engineering,
University of Michigan, USA

Abstract

This article describes design concept and material characteristics of a new ductile fiber reinforced cementitious composite referred to as ECC (Engineered Cementitious Composite). This particular ECC contains Polyvinyl Alcohol fiber and exhibits remarkably ductile tensile property with over 1% of tensile strain capacity. The high tensile strain performance of the ECC was found successfully utilized to improve the performance of structural elements via two demonstrative examples. First, it was found that ECC significantly enhanced shear performance of short span beam under cyclic loading. Second, ECC enables one to realize simple dry joint connecting panels with remarkably high shear load capacity for structural wall assembly. As conclusion, a strong potential of the ECC has been established to enhance the structural performance of seismic resistant elements.

Keywords: Pseudo-strain-hardening, Short fiber, Fiber composite, Shear element

1 Introduction

Random Short Fiber Reinforced Cementitious Composites (RSFRCC) have been improved to have significantly high ductility by utilizing micromechanics and fracture mechanics based design theory (Li 1993). These composites, often called Engineered Cementitious Composites (ECC), show Pseudo Strain Hardening (PSH) behavior with up to several percent of tensile strain capacity originated from numerous fine cracks developed perpendicular to the loading axis (multiple crack). The composites are expected to apply to structural element specifically to improve seismic resistant and durability (Maalej and Li 1995, Mishra and Li 1998, Naaman and Reinhardt eds. 1996).

This article demonstrates the effectiveness of a newly developed ECC in seismic resistant element. First, the properties of the new ECC containing high performance PVA (Polyvinyl Alcohol) fiber are briefly described. This PVA-ECC is considered cost-effective for practical applications and is therefore chosen for this demonstrative study. Next, the results of shear experiment on short span beam with the ECC subjected to cyclic loading are examined. As a second demonstration, the shear behavior of specially designed dry joint for ECC panel is presented. These experimental results lay the foundation for practical application of the new ECC for seismic elements.

2 Pseudo Strain Hardening Composite

Analyses of steady state crack propagation of a bridged crack leads to (Li 1993):

$$J_{tip} = \sigma_a \delta_a - \int_0^{\delta_a} \sigma_c(\delta) d\delta \qquad (1)$$

where J_{tip} is the crack tip toughness of the composite, σ_a is the steady state applied stress, δ_a is the corresponding crack opening displacement on the flat crack flanks, and σ_c is the crack bridging stress due to fiber. Relationship between σ_c and crack opening displacement δ, often referred to as bridging law, is the most important fundamental property of fiber composites. The bridging law for RSFRCCs was originally proposed by Li and Leung (1992), where σ_c is theoretically expressed as a function of fiber property, matrix property, and fiber/matrix interface property as well as δ.

$$\sigma_c = func.(\delta;\ \text{fiber property, matrix property, and fiber/matrix property}) \qquad (2)$$

During the event of multiple cracking, the next condition should be satisfied, otherwise a crack immediately opens up with degrading bridging stress σ_c.

$$\sigma_a < \sigma_{peak} \tag{3}$$

where, σ_{peak} denotes peak bridging stress in $\sigma_c - \delta$ relation. Combining Eqns. (1)-(3) completes design criteria for general ECCs. For the PVA-ECC used in the current experimental investigations, two important aspects, fiber rupture in bridging action and chemical bonding in fiber/matrix interface must be accounted for in the bridging law of Eqn. (2). These two aspects of PVA fiber bridging, observed in separate experiments, have been recently analyzed in detail by the authors (Kanda and Li 1998a; Kanda and Li 1998b), giving rise to design conditions for PVA-ECC.

The resulting PVA-ECC has 1-2 % of strain capacity with multiple cracking. This PVA-ECC employs matrix with water-by-cement-ratio of 45 % and sand ratio 40%. 2% volume of PVA fiber with 40 μm in diameter and 12 mm long is used for reinforcement. This fiber has approximately 800 MPa of tensile strength and 20000 MPa of elastic modulus. Details in this composite's design process can be found in Kanda and Li (1998c). Tensile and compressive test results with this composites are shown in Fig.1 (at 68 day age).

3 Shear behavior of Short Span Beam under Cyclic loading

3.1 Experimental Plan

Structural tests are conducted with ECC short-span beam reinforced with re-bars (R/ECC beam) subjected to cyclic loading. The test purpose is to ultimately apply this system to seismic resistant elements such as coupling beam and structural wall. This experiment was planned to uncover fundamental characteristics of R/ECC beam's shear behavior in comparison with regular Reinforced Concrete (R/C) beam serving as control, which employed plain concrete having similar compressive strength to the PVA-ECC. The configuration of beam specimens is shown in Fig.2, with 150 x 200 mm in section dimensions and 1500 mm in length. Loading span "a" is 400 mm for long beams and 200 mm for short beams. As in this figure, the experiment is conducted using what is generally known as the "Ohno shear beam". Cyclic loading is achieved by changing the horizontal location of supporting and loading points as shown by dotted triangles in Fig.2. To prevent flexural yielding of specimen and secure pure shear failure, 4% of longitudinal reinforcement

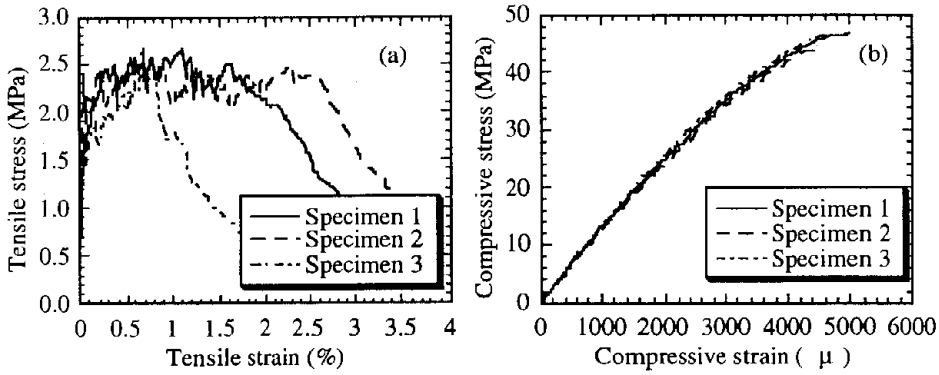

Fig. 1 Composite property of PVA-ECC, (a) in tension, (b) in compression

Table 1 Experimental Parameter

Beam specimen	Cement material	*1 M/QD	*2 p_w (%)	Failure mode
ECC-1-1	ECC	1	1	Shear comp.
ECC-1-0	ECC	1	0	Shear tens.
ECC-0.5-1	ECC	0.5	1	Shear comp.
ECC-0.5-0	ECC	0.5	0	Shear tens.
RC-1-1	Concrete	1	1	Shear comp.
RC-1-0	Concrete	1	0	Shear tens.

*1 Shear span to depth ratio
*2 Trans. reinf. ratio

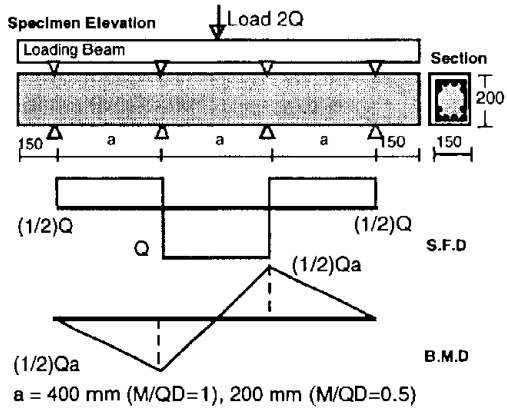

Fig. 2 Shear beam specimen (unit: mm)

was introduced. Loading are reversed at least two times, at initial cracking of ECC or concrete and at yielding of transverse reinforcement. Table 1 summarizes the outline of this experiment where a total of six specimens were tested, four were R/ECC beams and the other two were R/C beams as control. Experimental parameters are 1) type of cementitious material, ECC or plain concrete, 2) shear-span-to-depth ratio (M/QD), 1 or 0.5, and 3) transverse reinforcing ratio (p_w), 0 or 1 %. Specimens without transverse reinforcement are supposed to fail in shear tension while those with transverse reinforcement were designed to fail in shear compression. Therefore, the two levels of transverse reinforcing ratio correspond to the two anticipated failure modes.

3.2 Experimental Results and Discussion

3.2.1 Load-displacement relation

Fig.3 shows the comparison of load-displacement envelope curves obtained from the experiment. In this figure, open triangle indicates yielding of transverse reinforcement and solid triangle denotes peak point of envelope curves, which is defined as the ultimate point in this article. Only RC-1-0 specimen showed brittle shear failure but others exhibited similar ductile behavior in loading tests. Shear strength and ultimate displacement are summarized in Table 2. The effects of the first parameter, selection of cementitious material, are obvious by comparing ECC-1-0 to RC-1-0 in Fig.3 when shear tension is dominant. Furthermore, comparison of ECC-1-1 with RC-1-1 also reveals effects of using ECC when shear compression failure is dominant. These comparisons yield the following findings as summarized in Table 3.

1. Under shear tension failure mode, loading capacity is increased by 50 % and ultimate displacement is enhanced over 200% by using ECC instead of plain concrete.
2. Under shear compression failure mode, loading capacity is increased by 50 % while ultimate displacement is not very different by using ECC.

Thus it can be said that using ECC enhances shear performance while effects under shear tension failure mode is more remarkable than under shear compression failure mode.

Effects of the second parameter, combining transverse reinforcement with ECC, are revealed by contrasting ECC-1-1 with ECC-1-0 or ECC-0.5-1 with ECC-0.5-0 in Fig.3. In both cases, shear loading capacity is remarkably increased by 36—108 % while ultimate displacement is not significantly varied. Beams without transverse reinforcement, ECC-1-0 and ECC-0.5-0, showed rather ductile behavior. Hence this observation suggests that combining transverse reinforcement with ECC is effective in enhancing shear load resistance although ECC beams behave in ductile manner even without transverse reinforcement.

Effects of the third parameter, shear-span-to-depth-ratio M/QD, are revealed by contrasting ECC-1-1 with ECC-0.5-1 or ECC-1-0 with ECC-0.5-0 as in Table 3. In both cases, $p_w = 0$ and 1%, shear strength for M/QD = 0.5 is enhanced by 41—116% relative to that for M/QD = 1. Specimens with M/QD = 0.5 behave in similar ductile manner to those with M/QD = 1 while showing about 20% less ultimate displacement. It is generally known that short span elements with M/QD > 1 behave in brittle manner and difficult in improving such behavior. Therefore, it is worth emphasizing that ECC appears effective in preventing brittle shear behavior in very short-span beam even without transverse reinforcement.

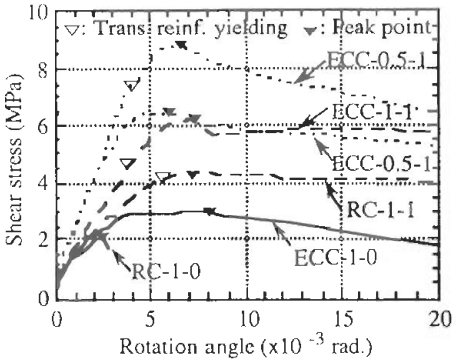

Fig. 3 Load-displacement envelope curves

Table 2 Experimental results

Specimen	Ult. Shear Capacity Q_u (kN)	Ult. Shear Stress τ_u(MPa)	Ult. Disp. δ_u(mm)	Ult. Rot. Angle R_u (rad.x10^{-3})
ECC-1-1	186	6.20	3.04	7.60
ECC-1-0	89.4	2.98	3.17	7.91
ECC-0.5-1	262	8.73	1.32	6.60
ECC-0.5-0	193	6.44	1.19	5.95
RC-1-1	128	4.27	2.91	7.28
RC-1-0	62.7	2.09	0.974	2.44

Table 3 Effect of parameter

Parameter	Condition	Improvement (%)		Comparison
		Q_u	R_u	
Using ECC	P_w=0%	42.6	225	RC-1-0 and ECC-1-0
	P_w=1%	45.3	4.47	RC-1-1 and ECC-1-1
Using Trans. Reinf.	M/QD=1	108	-3.95	ECC-1-0 and ECC-1-1
	M/QD=0.5	35.6	19.9	ECC-0.5-0 and ECC-0.5-1
Decreasing M/QD	P_w=0%	116	-24.8	ECC-1-0 and ECC-0.5-0
	P_w=1%	40.9	-13.2	ECC-1-1 and ECC-0.5-1

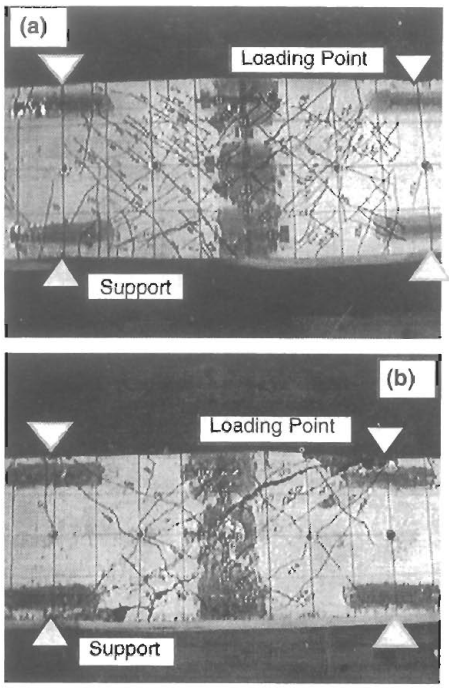

Fig. 4 Crack after loading, (a) ECC-1-1, and (b) RC-1-1

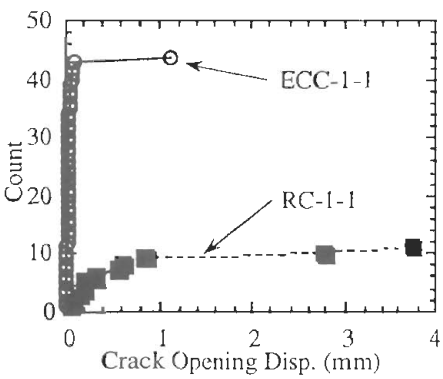

Fig. 5 Distribution of crack Opening Displacement

3.2.2 Cracking on specimen surface

The crack pattern on the specimen surface was significantly different between the R/C and R/ECC beams, which are illustrated in Fig.4 (a) and (b). Fig.4 (a) shows cracks on ECC-1-1 specimen after loading, in which much more cracks were generated with closer crack spacing than those on RC-1-1 specimen depicted in Fig.4 (b). This difference is summarized in Fig.5, which compares the distribution of crack opening displacement measured on the surface in specimens shown in Fig.4 (a) and (b). This crack examination was conducted along a line drawn perpendicular to the cracks near the center of the specimens, facilitated by optical microscope. Fig.5 demonstrates that cracks were observed in the R/ECC beam (ECC-1-1) approximately 4 times more than in the R/C beam (RC-1-1). Furthermore, crack opening displacement observed is significantly smaller in the R/ECC beam than the other even though both specimens experienced the same deformation in loading. These observations reflect ECC's material characteristics demonstrated in uniaxial tensile test, in which numerous fine cracks are densely generated and result in remarkable tensile strain capacity as implied in Fig.1. This much smaller crack opening may lead to advantages in R/ECC relative to R/C system in repairing damages by earthquake since fine cracks tend to be easily filled. In addition, spall resistant and cover protection is much more likely afforded by R/ECC elements than R/C elements.

4 ECC Panel Joint Subjected to Shear Loading

4.1 Panel Joint with ECC

ECC has outstanding potential to be applied to shear resistant element as indicated in the previous section. This section presents an additional demonstration of this potential in the retrofitting of structural walls to strengthen seismic resistance of building structures. Building retrofit construction usually demands heavy processes such as assembling large precast-concrete pieces and welding steel elements. This demand may be satisfied by using small pieces of ECC panel and assembling these with simple dry joint. The present investigation pursues this possibility by an experimental study of a new ECC panel joint. This new joint consists of ECC panels, a steel connecting plate and high-tension bolts as depicted in Fig.6. Four ECC panels sandwich a connecting plate and are directly fastened using high-tension bolts penetrating the panels and the plate. Panel material should bear compression stress highly concentrated under the bolts. To investigate compressive bearing capacity of ECC, indentation test with ECC panels are conducted. Following this test, shear loading test for this joint is performed using joint details shown in Fig.6.

4.2 Indentation Tests

The geometry of indentation test specimen is shown in Fig.7, which simulates a part of the panels connected with the proposed joint in Fig.6. The specimen has 300 x 300 mm of square plan and 75 mm thickness. The specimen's top and bottom surfaces were cast to be flat with mold surface. This bottom was fully supported by the flat surface of the testing apparatus. Loading was conducted by pushing an indentor, circular loading plate with steel, into the top surface of the specimen. The indentor has three sizes "d" = 30, 67 and 90 mm, such that the area of the indentor occupies 1, 5, and 10% of the specimen's top surface area respectively. This test employed ECC having the identical mix proportion to that used for the shear beam experiment in Section 3. In addition, the specimens with mortar were prepared as control, whose mix proportion is the same as an ECC's mortar part.

Specimens after failure are illustrated in Fig.8 for ECC and Fig.9 for mortar. Fig.8 (a) depicts surprisingly ductile behavior of an ECC specimen, into which the indentor was punched due to loading. Removing the indentor after loading yielded a hole as shown in Fig.8 (b). Many radial fine cracks were observed around the hole, which are extended from the hole to the specimen's perimeter. These evidences show "plastic" and damage tolerant property of ECC. On the other hand, mortar specimens showed typical brittle failure as shown in Fig.9, which illustrates the catastrophic failure with a couple of very sharp major fractures.

The difference in compressive bearing behavior is quantitatively revealed between ECC and mortar in Fig. 10 (a) and (b), which illustrate load-displacement relation obtained in the indentation tests. The comparison of these two figures reveals almost one order higher bearing displacement capacity of ECC specimens. In addition, ECC's load capacity is almost double that of mortar in the case with bearing area 1% while this ECC superiority is diminished with increasing bearing area. This difference in bearing performance implies that ECC can sustain much higher allowable bearing load than mortar due to higher material reliability as well as direct increase of load capacity. Being a brittle material, mortar's bearing performance may be expected to be sensitive to initial defects which inevitably exist in most cementitious materials. Being a damage tolerant material, ECC's strength may be fully utilized. This finding is reflected in designing the shear loading tests with the proposed ECC panel joint.

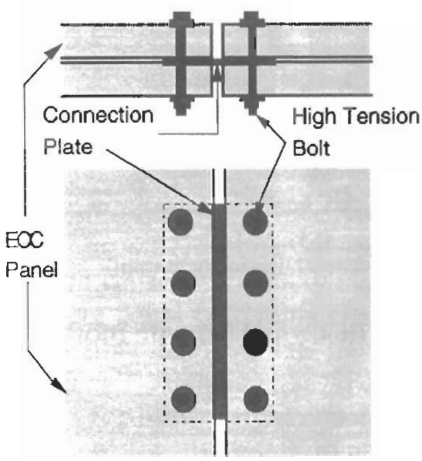

Fig. 6 Schematic of new dry joint

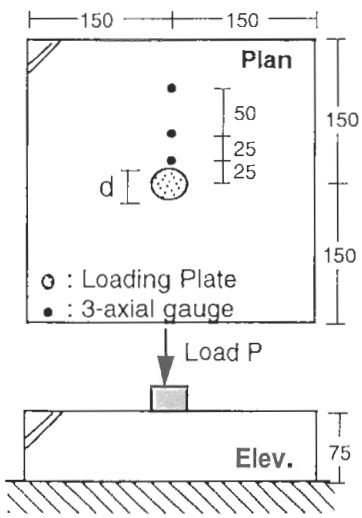

Fig. 7 Indentation specimen

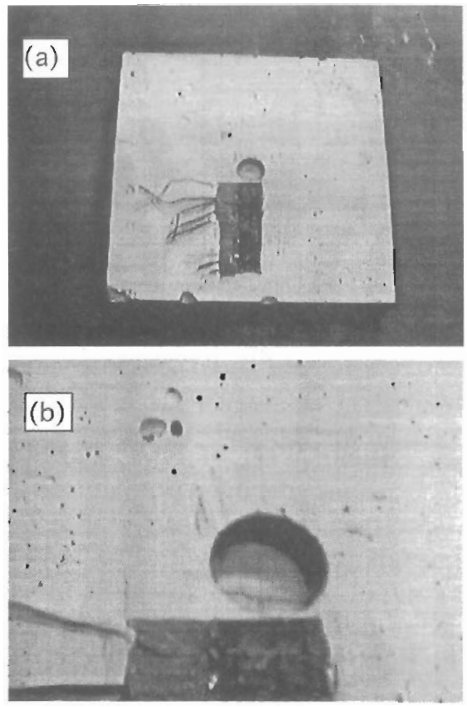

Fig. 8 Failure ECC specimen, (a) whole view, and (b) near indented part

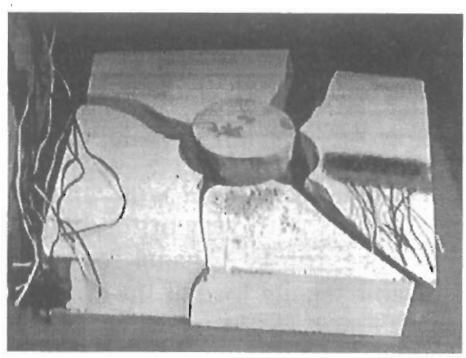

Fig. 9 Failure mortar specimen

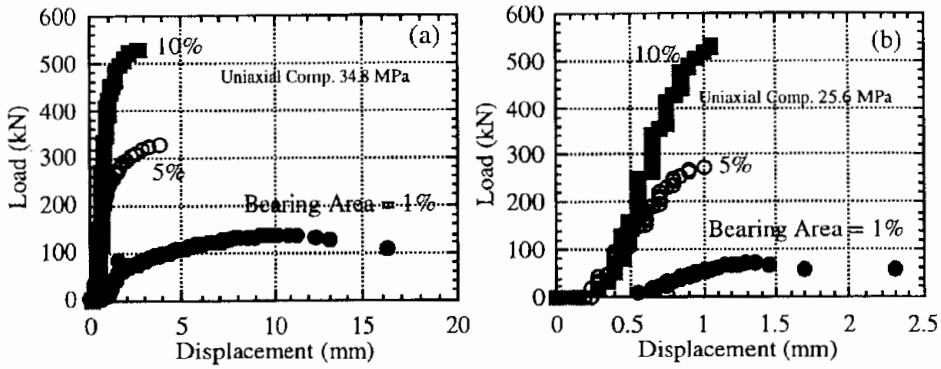

Fig. 10 Indentation test results, (a) with ECC, and (b) with mortar

4.3 Shear Test of ECC Panel Joint

4.3.1 Joint specimen preparation

A specimen for the shear joint tests is shown in Fig.11. Two specimens are prepared, one is with ECC and the other is with light weight concrete as control. The employed ECC has identical mix proportion to the one used in the compressive bearing tests, whose property is shown in Fig.1. The light weight concrete has 30.7 MPa of compressive strength at 69 days. All panels used for the specimen involve 0.75 % of longitudinal and transverse reinforcements. The joints in the specimen are fastened with high-tension bolts having 16 mm of nominal diameter and 164.6 kN of tensile load capacity. Bolt tension in the panels is introduced using torque wrench. Amount of the bolt tension load is controlled by monitoring axial strain via strain gauges embedded into a bolt. The other bolts are fastened to have the same torque as the bolt with the gauge.

Design bolt tension is determined by referring to the bearing test results summarized in Fig.10. Fig. 10 suggests that ECC can bear approximately 140 kN with significant ductility whereas mortar sustains about 70 kN with very brittle behavior in the case of the bearing area 1%. Therefore, for ECC panel specimen, bolt tension is introduced up to the allowable tensile load of the bolt, 103.9 kN. On the other hand, for light weight concrete, bolt tension is set to a half of ECC's considering expected brittle behavior. Elastic modulus of the bolt is measured as 207.6 GPa; hence the bolt's axial strain should attain approximately 3200 μ for ECC and 1600 μ for light weight concrete.

These design values of strain were actually introduced in the bolts. Strain became almost stable at 8 days after introducing tension but decreased about 20% compared with the initial strain for both ECC and light weight concrete specimens. Bolt strain was measured 2648 μ for ECC specimen and 1432 μ for light weight concrete specimen. As a

result, 86.3 kN per bolt (or 259 kN per joint) was introduced for ECC and 26.7 kN per bolt (or 140 kN per joint) was introduced for light weight concrete.

4.3.2 Result of joint shear test

Test results are summarized in Fig.12 and Fig.13, which illustrate the very different performance between ECC and light weight concrete joints. Fig.12 shows the load-displacement results in the shear loading tests, where the ECC joint reveals close to double the shear loading capacity of the light weight concrete joint. Indeed, the ECC joint showed higher loading capacity than any other conventional joints with the light weight concrete panel (Akiyama et al. 1997). The peak load in Fig.12 allows us to calculate the average shear stress transferred from the joints to the panels. This shear stress is calculated as about 4 MPa for ECC panels and 2 MPa for light weight concrete panels. 4 MPa of shear strength may be sufficient for the panel joint in structural walls, whose allowable shear stresses are usually much less than 4 MPa according to Japanese building code (AIJ 1988). Furthermore, the genuine shear resistance of the ECC joint could be higher than the observed in the test. This is because the ECC joint specimen did not fail at joint part but near supporting point as explained in the next.

The failure mode of the joint specimens is also different between ECC and light weight concrete, which is compared in Fig.13 (a) and (b). The ECC joint specimen exhibited almost no visible damage in joint part, but was crushed near the support, indicated by the hatched region in Fig.13 (a). This crushing appears due to highly concentrated compression at support. Therefore, it can be said that ECC's joint strength obtained in this experiment is a lower bound value. In contrast, the light weight concrete joint specimen failed completely in the joint region. Major cracks were initiated at bolt holes and eventually connected those holes. Apparently, the high stress concentration near the holes, which are considered as a kind of defect, led to the fracture failure of the joint. The high damage tolerant characteristics of ECC prevented this kind of failure, even when subjected to rather high shear stress like 4 MPa.

5 Conclusion

This article described 1) briefly the design concept and material characteristics of a new ECC and 2) the demonstrative application of the ECC to seismic resistant elements via experimental results. Following the composite design theory summarized here, over 1% of tensile strain capacity was achieved in the new ECC incorporating PVA fiber commonly used in construction industry. The high tensile strain performance of the

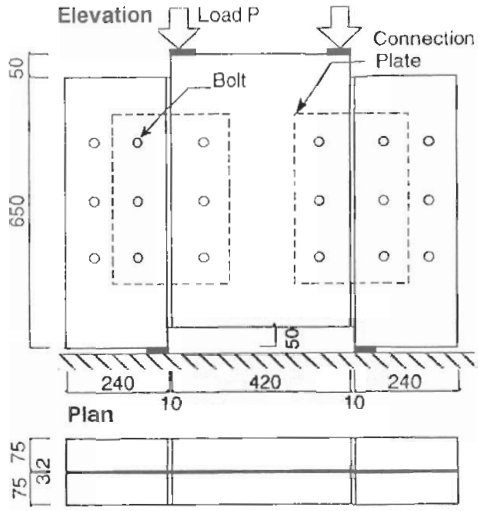

Fig. 11 Specimen of shear joint test

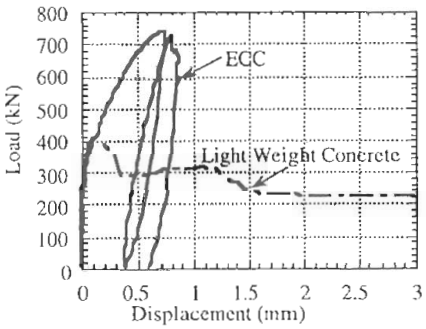

Fig. 12 Shear joint test result

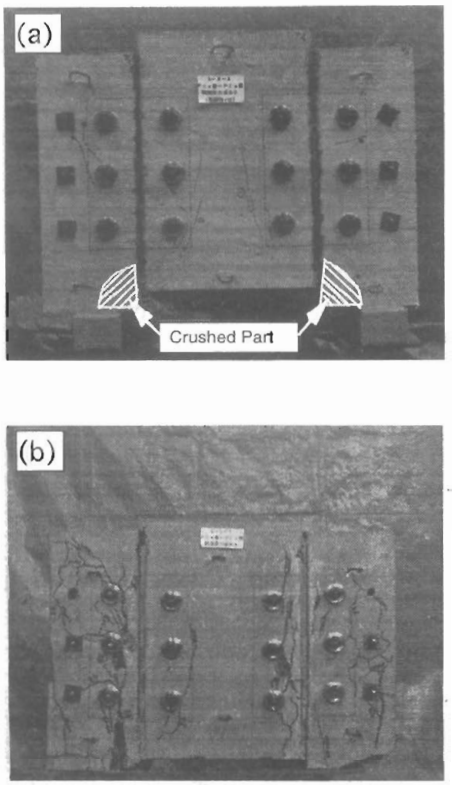

Fig. 13 Shear joint specimen after loading, (a) ECC and (b) Concrete

ECC was found successfully utilized to improve structural element performance. For shear behavior of short span beam, ECC was found to significantly enhance the shear resistance when shear compression is dominant. The effects of ECC are even more remarkable when shear tension is dominant, where deformation capacity as well as the shear resistance are substantially improved. Furthermore, applying ECC enables one to realize simple dry joint connecting panels with high shear load capacity needed for structural wall assembling. In conclusion, the potential of ECC for enhancing the structural performance of seismic resistant elements has been unequivocally established by this series of experimental investigation results.

6. Acknowledgment

Special thanks are due to Dr. H. Horii and Dr. P. Kabele at the University of Tokyo for their valuable technical advice. Mr. T. Hamada at Kuraray Cooperation (Osaka, Japan) is acknowledged for fiber material supply.

7. References

Akiyama, S., Yamada, T., and Kanda T.(1997) Shear Test of Precast Concrete Panel Joints, **Transactions for Annual Meeting of AIJ,** Architectural Institute of Japan, Vol. Structure IV, 427-428, July (in Japanese)

Architectural Institute of Japan (1988) Standard for Structural Calculation of Reinforced Concrete Structures, 207-234 (in Japanese).

Kanda, T, and Li, V. C. (1998a) Interface Property and Apparent Strength of High-Strength Hydrophilic Fiber in Cement Matrix, **J. of Materials in Civil Engineering**, ASCE, 10(1), 5-13, Feb.

Kanda, T, and Li, V. C. (1998b) Effect of Apparent Fiber Strength and Fiber-Matrix Interface on Tensile Property of Cementitious Composites, **J. of Engineering Mechanics**, ASCE (under review)

Kanda, T, Li, V. C., and Hamada, T. (1998c) Material Design and Development of High-Ductility Composite Reinforced with Short Random Polyvinyl Alcohol Fiber, **Proceedings of the Japan Concrete Institute**, 20 (to be appeared, in Japanese)

Li, V. C. (1993) From Micromechanics to Structural Engineering -The Design of Cementitious Composites for Civil Engineering Applications, **J. Struct. Mech. Earthquake Eng.**, Japan Society of Civil Engineers, 10(2), 37-48, July

Maalej, M., and V.C. Li (1995) Introduction of Strain Hardening Engineered Cementitious Composites in the Design of Reinforced Concrete Flexural Members for Improved Durability, **American Concrete Institute Structural J.**, 92(2), 167-176, March-April.

Mishra, D. K., and Li, V. C. (1998) Performance of a Ductile Plastic Hinge Designed with an Engineered Cementitious Composite, **Material and Structures**, RILEM (under review)

Naaman, A. E. and Reinhardt, H. W. eds., (1996) **High Performance Fiber Reinforced Cement Composites,** 2, Chap. 8, E.& F.N. Spoon, London, 291-348.